

# Experimental study on thermal behaviors in square-duct with 45° discrete V-finned tape inserts with V-tip pointing downstream

Supattarachai Suwannapan\*, Kanchit Rongchai, Sura Tundee

Department of Mechanical Engineering, Faculty of Engineering, Rajamangala University of Technology Isan, Khonkaen Campus, 150 Srichan Rd., Muang, Khonkaen 40000, Thailand

\*Corresponding author, E-mail address: oak\_su@hotmail.com

Tel.:+66 43-336-370, Fax.: +66 43-237-483

## Abstract

In the development of high performance compact heat exchangers, various flow tabulators used in the purpose of enhancing heat transfer have been studied. This article presents a new experimental study on thermal performance enhancement in a constant heat fluxed square duct inserted diagonally with a 45° discrete V-finned tape with V-tip pointing downstream (45° DFTVD). The study was conducted by varying the airflow rate through the tested square duct fitted with the 45° DFTVD for Reynolds number from 4000 to 25000. Various relative fin heights and pitches were tested to investigate the effect of the 45° DFTVD at on heat transfer and pressure drop. Heat transfer and pressure drop were presented in terms of Nusselt number and friction factor respectively. Several V-finned tape characteristics were introduced such as fin-to-duct height ratio or blockage ratio ( $BR=e/H=0.075, 0.1, 0.15$  and  $0.2$ ), fin pitch to duct height ratio ( $PR=P/H=0.5, 1.0, 1.5$  and  $2.0$ ) and fin attack angle,  $\alpha =45^\circ$ . The results have shown that the heat transfer and friction factor values with the 45° DFTVD increase with increasing  $BR$  but with decreasing  $PR$ . The highest heat transfer and friction factor were observed at  $BR=0.2$  and  $PR=0.5$  whereas the highest thermal enhancement factor was at  $BR=0.1$  and  $PR=1.5$ . Considering measurement uncertainties, it was also found that changing the V-tip direction to pointing upstream results in an insignificant increase of 3% in thermal enhancement factor.

**Keywords :** discrete V-fins, heat transfer, heat exchanger, thermal enhancement, square duct

## 1. Introduction

Heat exchangers are essential in many engineering applications. To achieve high thermal efficiency, many design parameters such as heat transfer rate, pressure penalty, structure and size need to be considered. Heat exchangers were originally introduced as a plain or smooth-surfaced device. However, due to the quest for higher performance, compactness and efficiency, several heat transfer enhancement techniques have been developed. The improvement techniques can be classified into two categories: passive and active. With no external work requirement to enhance heat transfer, the passive method takes advantage of specially designed surface characteristics of the duct together with the use of a special fluid. There are many ways in which passive techniques are implemented such as surface coating, increase surface roughness, increase surface areas, coiled tubes, displaced inserts, surface tension and fluid additives. On the other hand, the active method requires an external power source to induce surface vibration or fluid vibration which then increases the heat transfer rate. Extensive research has previously been conducted on heat transfer, pressure drop and thermal performance characteristics of heat exchangers using enhancing devices such as ribs, fins, baffles and winglets.

Detailed reviews have been widely reported by many authors. Liu et al. [1] experimentally studied heat transfer characteristics in steam-cooled rectangular channels with two opposite rib-roughened walls. They tested two attack angles ( $\alpha$ ) of  $45^\circ$  and  $60^\circ$  and reported that the average Nusselt number for the channel was

higher for  $45^\circ$ . Sriromreun et al. [2] investigated the influence of baffle turbulators on heat transfer augmentation in a rectangular channel. In the experiment, the Nusselt number, friction factor and thermal performance enhancement factor for in-phase  $45^\circ$  Z-baffles were found to be considerably higher than the out-phase  $45^\circ$  Z-baffle. A numerical study of a finned flat tube heat exchanger with discrete double inclined ribs by Song et al. [3] shows that heat transfer is enhanced by secondary flows around the ribs and a series of vortices generated downstream of the ribs, including the main vortices, induced vortices and corner vortices. The Nusselt number for the attack angle of  $\alpha = 45^\circ$  was larger than for  $\alpha = 30^\circ$  and  $\alpha = 60^\circ$ . The friction factor increased with the attack angle. Skullong and Promvonge [4] presented an experimental study on heat transfer and flow friction characteristics in a solar air heater channel fitted with delta-winglet. They reported that the  $30^\circ$  delta-winglet placed only on the upper wall yielded the best thermal performance. Promvonge [5] presented the turbulent forced convection heat transfer and friction loss behaviours for airflow through a channel fitted with a multiple 60o V-baffle turbulator. Peng et al. [6] studied experimental and numerical convection heat transfer in a channel with  $90^\circ$  ribs and V-shaped ribs. The results showed that both the  $90^\circ$  ribs and V-shaped ribs enhanced the convection heat transfer compared with a flat wall without ribs, although at the expense of increasing pressure drop. Promvonge et al. [7] numerically investigated laminar flow and heat transfer characteristics in a three-dimensional isothermal wall square channel fitted with inline  $45^\circ$  V-

shaped baffles on two opposite walls. The baffled channel flow showed a fully developed periodic flow and heat transfer profile for  $x/D \approx 8$  downstream of the inlet. It was apparent that the longitudinal counter-rotating vortex flows created by the V-baffle can induce impingement attachment flows over the walls resulting in greater increase in heat transfer over the test channel. Gupta et al. [8] studied local heat transfer distributions in a double wall ribbed square channel with  $90^\circ$  continuous,  $90^\circ$  saw tooth profiled and  $60^\circ$  V-broken ribs. They found that the heat transfer enhancements using  $60^\circ$  V-broken ribs were higher than  $90^\circ$  continuous ribs. Chompookham et al. [9] experimentally investigated the effect of combined wedge ribs and winglet type vortex generators on heat transfer and friction loss behaviors in a channel, two types of wedge ribs are introduced: wedge ribs pointing downstream and pointing upstream. Skullong et al. [10] presented an experimental study on turbulent flow and heat transfer characteristics in a solar air heater channel fitted with combined  $45^\circ$  wavy-rib and groove turbulators. They reported that the combined rib-groove on both the upper and lower walls provided the highest heat transfer rate and friction factor in comparison with ribbed wall. Min et al. [11] experimentally investigated the influence of a modified rectangular longitudinal vortex generator obtained by cutting off the four corners of a rectangular wing on fluid flow and heat transfer characteristics in a rectangular channel. Results showed that the modified rectangular wing pairs had better flow and heat transfer characteristics than rectangular wing pair. As far as heat transfer in ducts is concerned, Hans

et al. [12] experimentally investigated the effect of multiple V-rib roughness on heat transfer coefficient and friction factor in an artificially roughened solar air heater duct. Eiamsa-ard and Promvong [13] studied the effects of combined rib-grooved turbulators on heat transfer and friction characteristics in a rectangular duct. In the experiments, three types of rib-groove arrangements were tested: rectangular-rib and triangular-groove, triangular-rib and rectangular-groove, and triangular-rib and triangular-groove were introduced. They reported that the triangular-rib with triangular-groove gave the highest thermal performance amongst all pitch ratios studied. In the case of square ducts, Eiamsa-ard et al. [14] experimentally investigated the effects of wire coil elements on heat transfer and flow friction characteristics in a square duct. Apart from the full-length coil, 1D and 2D length coil elements placed in tandem inside the duct with various free-space lengths were introduced to reduce the friction loss. The experimental results showed that the use of wire coil inserts for the full-length coil, 1D and 2D coil elements with a short free-space length leads to a considerable increase in heat transfer and friction loss over the smooth duct with no insert. The full-length wire coil provided higher heat transfer and friction factor than the tandem wire coil elements under the same operating conditions. Promvong et al. [15, 16] experimentally investigated heat transfer augmentation in a square duct with insertion of combined V-fins and twisted tapes. Their results reveal that thermal performance of the combined V-finned and twisted tape is considerably higher than that of the twisted tapes alone. Promvong et al. [17, 18] studied the

turbulent flow and heat transfer characteristics in a square duct fitted diagonally with 30° angle-finned tapes. A more recent and relevant study was reported by Noothong et al. [19]. They investigated thermal performance enhancement in a square duct inserted with discrete V-finned tapes (DFT), with V-tip pointing upstream. The experimental results show that the heat transfer and friction factor values with the DFT increase with increasing blockage ratio but with decreasing pitch ratio. Their numerical study shows that the DFT gives rise to two longitudinal counter-rotating vortices along the duct that help increase turbulence intensity. The mechanism of the heat transfer enhancement is the impingement reattachment flow of the longitudinal vortex flows. They reported that the new technique provides higher thermal performance than wire-coil/twisted-tape inserts.

As a continuation to the above studies, the present work focuses on the experimental investigation of a square duct heat exchanger inserted diagonally with a 45° DFTVD which has never been reported previously. Our study directly corresponds to the work by Noothong et al. [19] where the use of a 45° discrete V-finned tape (DFT) has first been reported. The experimental setup is explained and the results are presented together with analysis and discussion. Comparison with the previous study was made. Conclusions are drawn.

## 2. Experimental Setup

A schematic diagram of the experimental setup is presented in Fig. 1. The system consists of a high-pressure blower, an orifice flow meter, a settling tank, and a square duct test section. The overall length of the duct was 3000 mm,

comprising an entrance section of 2000 mm and a test section of 1000 mm ( $L$ ). The test section of the square duct was made of an aluminium plate having a thickness of 3 mm and cross sectional area of 2025 mm<sup>2</sup> (45×45 mm).

An AC power supply provided energy for heating all of the four walls of the test section and maintaining a uniform surface heat flux condition. Air as the working fluid was forced through the system by a 1.45 kW high-pressure blower. The air flow rate was controlled by an inverter and was measured using an orifice plate. The orifice plate was calibrated by hot-wire and vane-type anemometers. The pressure drop across the orifice was measured using an inclined manometer. The axial temperature distributions along the test section were measured by twenty-eight thermocouples. Two thermocouples were positioned at the entrance and the exit of the duct to measure the inlet and outlet temperatures. All thermocouples were type-K having 1.5 mm diameter wires. All measured temperature values were fed into a data logger and recorded via a personal computer. Two static pressure taps were located at the top walls to measure axial pressure drops across the test section. This pressure drop was required in order to calculate the friction factor. They were located at the centre line of the duct. The first pressure tap was located at the entrance of the test section and the other was located at the exit of the test section. The pressure drop was measured by a digital differential pressure transducer. The uncertainty analysis in the data calculation was based on Ref. [20]. The maximum uncertainties of non-dimensional parameters were ±5% for Reynolds number, ±7% for Nusselt number and

$\pm 9\%$  for friction factor. Figure 2 schematically illustrates the test section fitted with  $45^\circ$  discrete V-fins placed on a straight tape. The diagonal straight tape was made of an aluminium sheet with dimensions of  $63 \times 1200 \times 0.5$  mm. The V-fins made of a 0.3 mm aluminium strip were attached on both sides of the straight tape.

and 0.2, respectively. Fin parameters tested were four fin pitch to duct height ratios,  $PR=P/H=0.5, 1.0, 1.5$  and 2.0, and a single attack angle ( $\alpha$ ) of  $45^\circ$ , with V-tip pointing downstream.

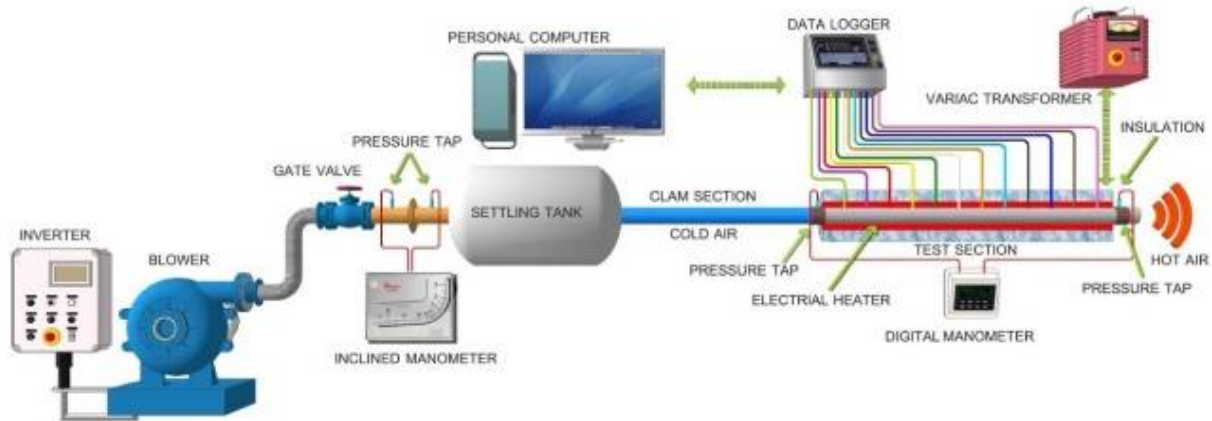


Fig. 1. Schematic diagram of the experimental apparatus.

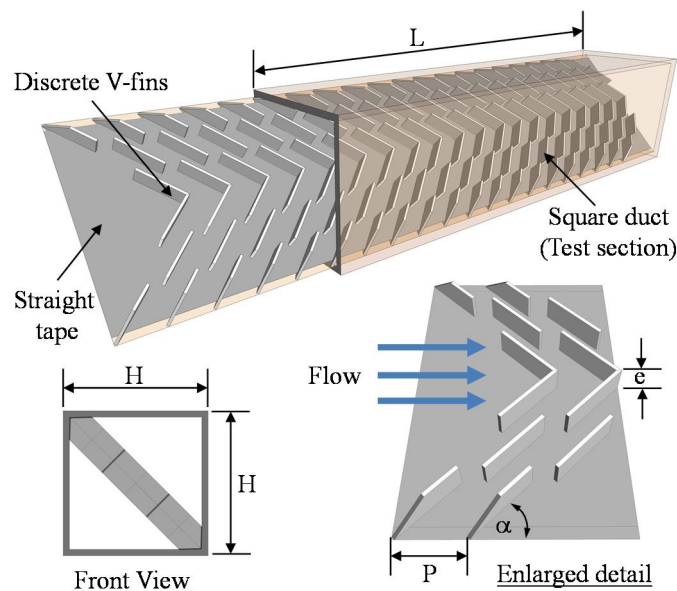


Fig. 2. Test section with the  $45^\circ$  discrete V-finned placed on a straight tape..

Four fin heights, symbolized as  $e$ , were tested: 3.375, 4.5, 6.75 and 9 mm, all of which having a thickness ( $t$ ) of 0.3 mm. The equivalent fin to duct height ratios,  $BR=e/H$  are hence, 0.075, 0.1, 0.15

### 3. Data analysis

The objective of the experiment is to investigate heat transfer, pressure drop and thermal performance of the heat exchanger

square duct with the 45° DFTVD. Following similar analysis presented in Noothong et al. [19], the experimental results of the heat transfer and pressure drop are presented as dimensionless Nusselt numbers and friction factors respectively. The average heat transfer coefficients are evaluated from the measured temperatures and heat inputs, with heat added uniformly to the fluid ( $Q_{air}$ ) and the temperature difference between the surface and the fluid ( $\tilde{T}_s - T_b$ ). The average heat transfer coefficient is evaluated from the experimental data via the following equations:

$$Q_{air} = Q_{conv} = \dot{m}C_p(T_o - T_i) \quad (1)$$

$$h = \frac{Q_{conv}}{A(\tilde{T}_s - T_b)} \quad (2)$$

in which,

$$T_b = (T_o + T_i)/2 \quad (3)$$

and

$$\tilde{T}_s = \sum T_s/28 \quad (4)$$

The term  $A$  is the convective heat transfer area of the heated duct wall whereas  $\tilde{T}_s$  is the average surface temperature obtained from local surface temperatures along the axial length of the heated duct. Then, the average Nusselt number is written as

$$Nu = \frac{hD_h}{k} \quad (5)$$

The Reynolds number based on the duct hydraulic diameter ( $D_h$ ) is given by

$$Re = UD_h/\nu \quad (6)$$

where  $A_c$  is the cross-sectional area and  $P_w$  is the wetted perimeter of the cross section. The friction factor ( $f$ ) is evaluated by

$$f = \frac{2}{(L/D_h)} \frac{\Delta P}{\rho U^2} \quad (7)$$

where  $\Delta P$  is the pressure drop across the test section and  $U$  is the mean air velocity of the duct. All thermo-physical properties of air are determined at the overall bulk air temperature from Eq. (3).

The thermal enhancement factor ( $\eta$ ) defined as the ratio of the heat transfer coefficient of an augmented surface,  $h$  to that of a smooth surface,  $h_0$ , at a constant blowing power [21] is given by

$$\eta = \frac{h}{h_0} \Big|_{bp} = \frac{Nu}{Nu_0} \Big|_{bp} = \left( \frac{Nu}{Nu_0} \right) / \left( \frac{f}{f_0} \right)^{1/3} \quad (8)$$

## 4. Results and Discussion

### 4.1 Validation of smooth square duct

The experimental results of the Nusselt number ( $Nu$ ) and friction factor ( $f$ ) obtained from the present smooth duct are compared with the correlations of Dittus-Boelter, Gnielinski, Blasius and Petukhov [22] for turbulent flow in ducts. The correlations of the Nusselt number postulated by Dittus-Boelter, and Gnielinski are shown in Eq. 9 and Eq. 10, respectively and the friction factor correlations by Blasius and Petukhov are given in Eq. 11 and Eq. 12 respectively.

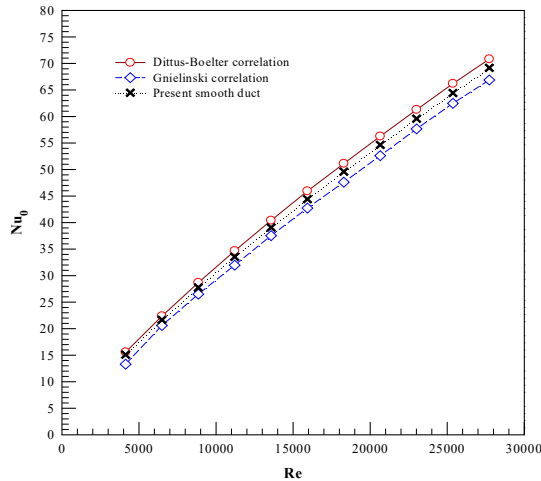
$$Nu = 0.023 Re^{0.8} Pr^{0.4} \quad (9)$$

$$Nu = \frac{(f/8)(Re - 1000)Pr}{1 + 12.7(f/8)^{1/2}(Pr^{2/3} - 1)} \quad (10)$$

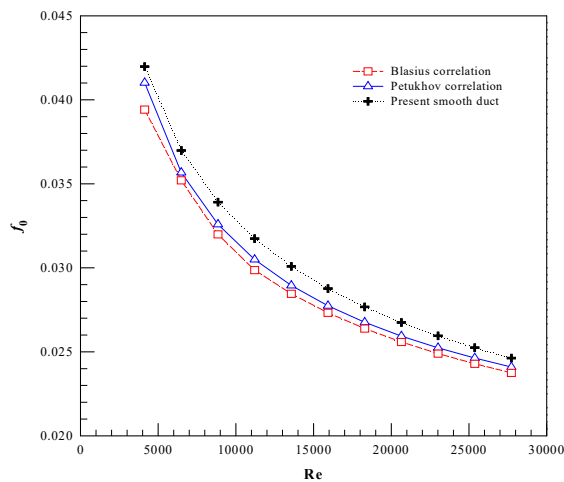
$$f = 0.316 Re^{-0.25} \quad (11)$$

$$f = (0.79 \ln Re - 1.64)^{-2} \quad (12)$$

Figures 3a and 3b show the comparison between the Nusselt number and friction factor obtained from the present work with those from correlations from Eqs. 9-12.



(a)



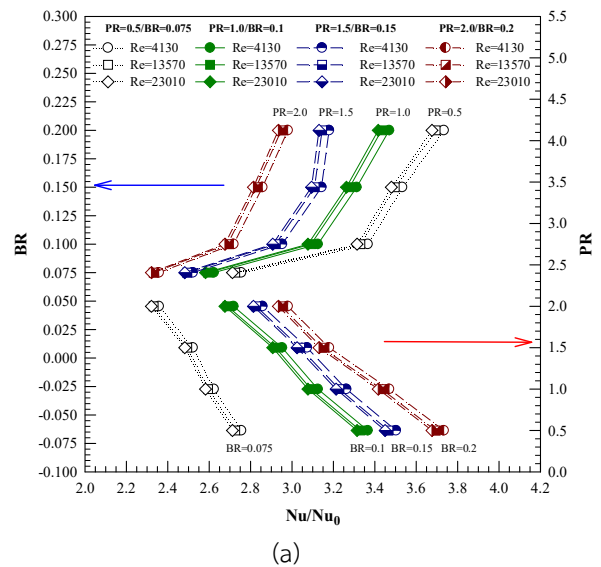
(b)

Fig. 3. Validation of (a)  $Nu_0$  and (b)  $f_0$  with  $Re$  for smooth duct.

As seen from the figures, both of the present results agree well within  $\pm 5\%$  with the correlation data.

#### 4.2 Heat transfer rate and pressure drop behaviours

In Fig. 4a, it can be observed that the inserted duct yields considerable heat transfer enhancement following a similar trend in comparison with the smooth duct and thus, the  $Nu$  increases with increasing  $Re$ . When air flows into the smooth duct, there is a boundary layer - an undisturbed air layer just above the duct's surfaces through which heat transfer rate is relatively low. The thickness of the boundary layer can be broken or reduced by using the  $45^\circ$  DFTVD. It creates turbulence in the duct which enhances momentum and energy transfer, thereby increasing convective heat transfer rate. On the other hand, the  $45^\circ$  DFTVD unavoidably increases surface friction and hence pressure loss. It is visible in Fig. 4b that the use of the vortex generators leads to a substantial increase in friction factor ( $f$ ) above the smooth duct case. However, there is a decreasing trend in friction factor with increasing  $Re$ .



(a)

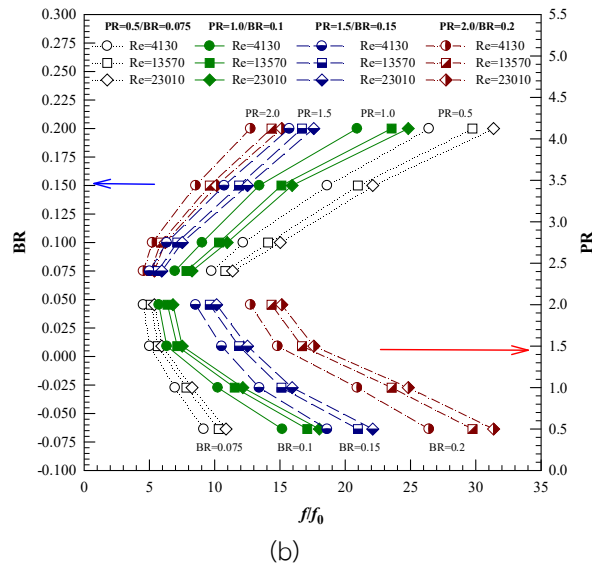


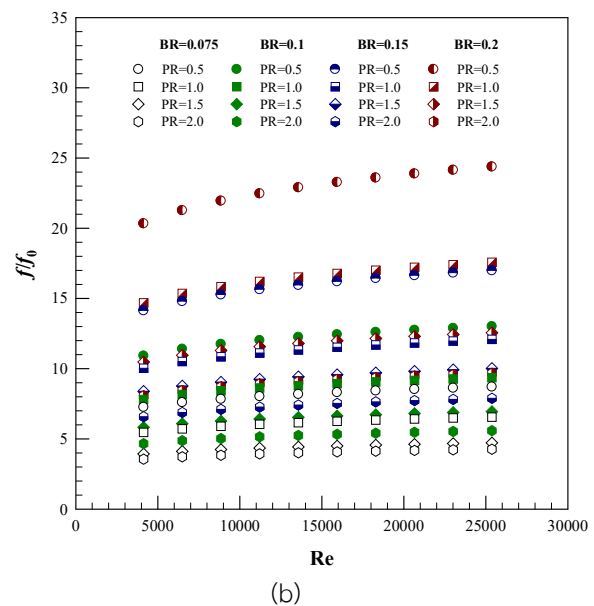
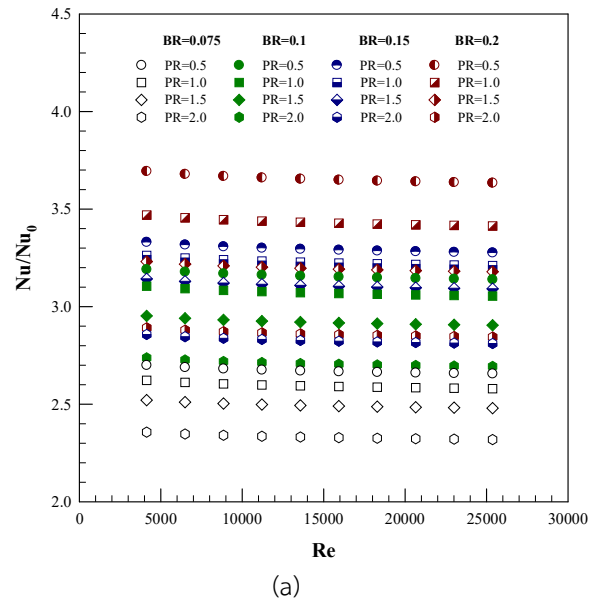
Fig. 5. Variation of (a)  $Nu/Nu_0$  and (b)  $ff_0$  with  $PR$  and  $BR$  for  $45^\circ$  DFTVD.

#### 4.4 Performance evaluation

The  $Nu/Nu_0$ ,  $ff_0$  and  $\eta$  for the  $45^\circ$  DFTVD plotted against  $Re$  is displayed in Fig. 6a, 6b and 6c, respectively. In the figure, it can be seen that the  $Nu/Nu_0$  and the  $\eta$  tend to decrease with increasing  $Re$  while the  $ff_0$  shows an opposite trend. Fig. 6a and 6b, it is found that the  $45^\circ$  DFTVD yields the values of  $Nu/Nu_0$  and  $ff_0$  at about 2.84-3.69, 2.81-3.33, 2.69-3.11 and 2.32-2.70; and 8.07-24.38, 6.58-16.99, 4.66-13.01 and 3.56-8.71 times above the smooth duct for  $BR=0.2$ , 0.15, 0.1 and 0.075 respectively depending on  $PR$  and  $Re$ . The V-fin vortex generators with  $PR=0.5$  and  $BR=0.2$  provides the highest  $Nu/Nu_0$  and  $ff_0$  or about 28-83% and 6-36% higher than those at other  $BR$ s and  $PR$ s respectively.

The variation of the thermal enhancement factor ( $\eta$ ) with Reynolds number ( $Re$ ) for the  $45^\circ$  DFTVD is depicted in Fig. 6c. In the figure,  $\eta$  decreases with increasing  $Re$  for all cases. The maximum thermal enhancement factor of about

1.66 is found when  $BR=0.1$  and  $PR=1.5$  at  $Re=4130$ . Thus, the optimal parameter of the present work is  $BR=0.1$  because at this point, the highest  $\eta$  is obtained regardless of the  $PR$ . The  $45^\circ$  DFTVD yields the values of  $\eta$  at about 1.25-1.47, 1.27-1.56, 1.35-1.66 and 1.29-1.60 depending on  $PR$  and  $Re$ , for  $BR=0.2$ , 0.15, 0.1 and 0.075 respectively. The value of  $\eta$  at  $BR=0.1$  and  $PR=1.5$  is about 2-18% higher than all other cases.



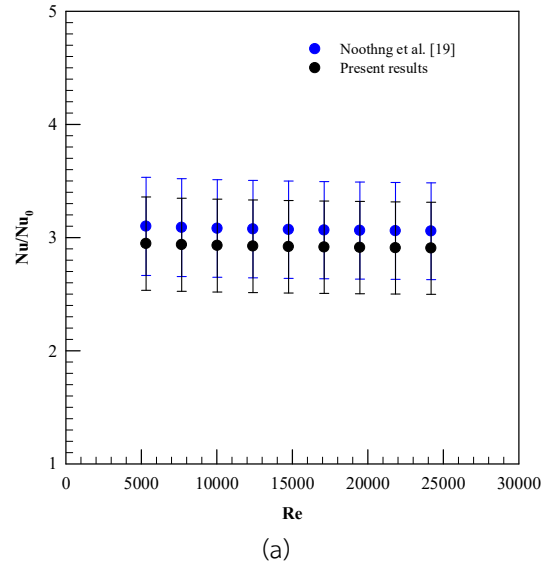
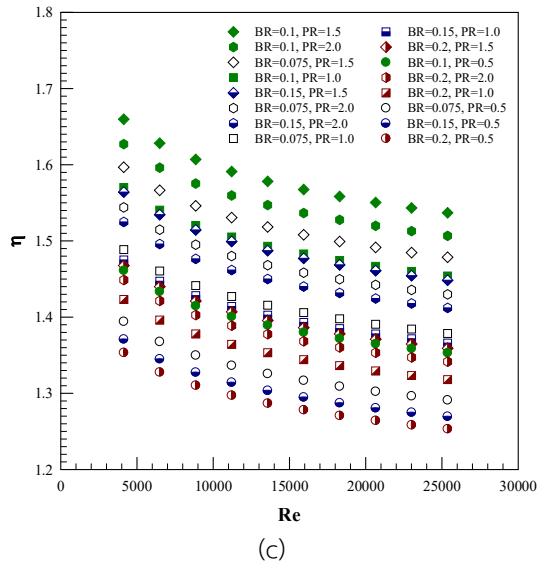


Fig. 6. Variation of (a)  $Nu/Nu_0$ , (b)  $f/f_0$ , and (c)  $\eta$  with  $Re$  for  $45^\circ$  DFTVD.

#### 4.5 Effect of V-tip direction arrangement

The present results are compared with the similar study by Noothong et al. [19] where a  $45^\circ$  DFT with V-tip pointing upstream in a square duct was investigated. The conditions used in our study were identical the previous work. The number of fins on the DFTVD,  $BR$  and  $PR$  values, the square duct and the flow conditions were identical, thus enabling us to study the direct effect of V-tip pointing upstream and downstream on the DFTVD performance.

At this stage, it goes without saying that measurement uncertainty should come into play. The general theory of error propagation in Eq. 13 was employed when estimating uncertainties in  $Nu/Nu_0$ ,  $f/f_0$ , and  $\eta$  where  $u(y)$  and  $u(x_i)$  are uncertainties in variables  $y$  and  $x_i$  respectively [23]. The method of finite difference was used when calculating derivatives.

$$u(y)^2 = \sum_{i=1}^N \left( \frac{\partial y}{\partial x_i} \right)^2 u(x_i)^2 \quad (13)$$

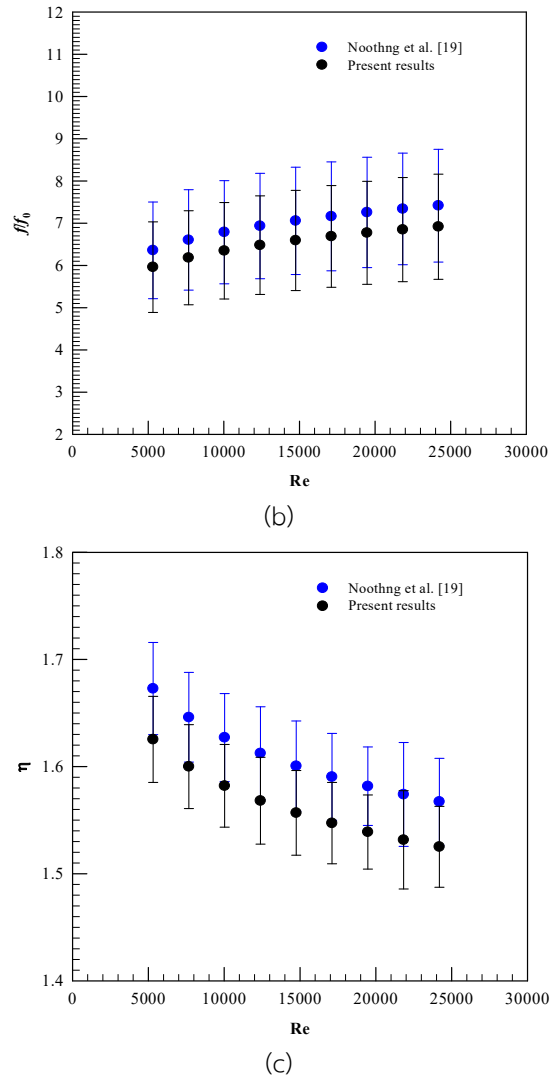


Fig. 7. Comparison between the present results and Noothong et al. [19] of (a)  $Nu/Nu_0$ , (b)  $f/f_0$ , and (c)  $\eta$ .

For the sake of clarity, only the case with the highest thermal enhancement factor from the current and Noothong et al's results were selected for comparison. Figures 7a, 7b and 7c compare the data points for  $Nu/Nu_0$ ,  $f/f_0$ , and  $\eta$  with the estimated error bars for the current and Noothong et al's studies as functions of Reynolds number. First of all, it was found that the highest thermal enhancement factor was achieved when  $BR = 0.1$  and  $PR = 1.5$  for both V-tip pointing upstream and downstream. This shows that such fin parameters were optimal regardless of V-tip direction. Highest  $\eta$ 's were achieved at the low end of the Reynolds realm and show a downtrend as  $Re$  increases. On average, changing the V-tip direction from pointing downstream to upstream results in an approximately 3% increase in thermal enhancement factor. However, the increase is insignificant compared with the equal propagated error of  $\pm 3\%$  for both the current and previous works.

#### 4.6 correlations for Nu number and f

Heat transfer and pressure drop in the uniform heat-fluxed square duct with the  $45^\circ$  DFTVD were measured and presented in terms of Nusselt number ( $Nu$ ) and friction factor ( $f$ ) as functions of Reynolds number as illustrated in Fig. 8a and 8b. For clarity of comparison, the empirical correlations for Nusselt number and friction factor as functions of Reynolds number ( $Re$ ), Prandtl number ( $Pr$ ), blockage ratio ( $BR$ ) and pitch ratio ( $PR$ ) have been used. For  $BR=0.075, 0.1, 0.15$  and  $0.2$ ; and  $PR=0.5, 1.0, 1.5$  and  $2.0$ ; and for  $Re$  ranging from 4000 to 25,000, the empirical correlations are shown in Eqs. 14 - 15.

$$Nu = 0.122Re^{0.790}Pr^{0.4}BR^{0.245}PR^{-0.114} \quad (14)$$

$$f = 11.412Re^{-0.180}BR^{0.941}PR^{-0.584} \quad (15)$$

To demonstrate the representativeness of the correlations in Eqs. 14-15, the predicted Nusselt number and friction factor are plotted against the measured data as shown in Fig. 8a and 8b. It can be seen that the experimental data points fall within  $\pm 10\%$  and  $\pm 11\%$  of the predictions for the  $Nu$  and  $f$  respectively.

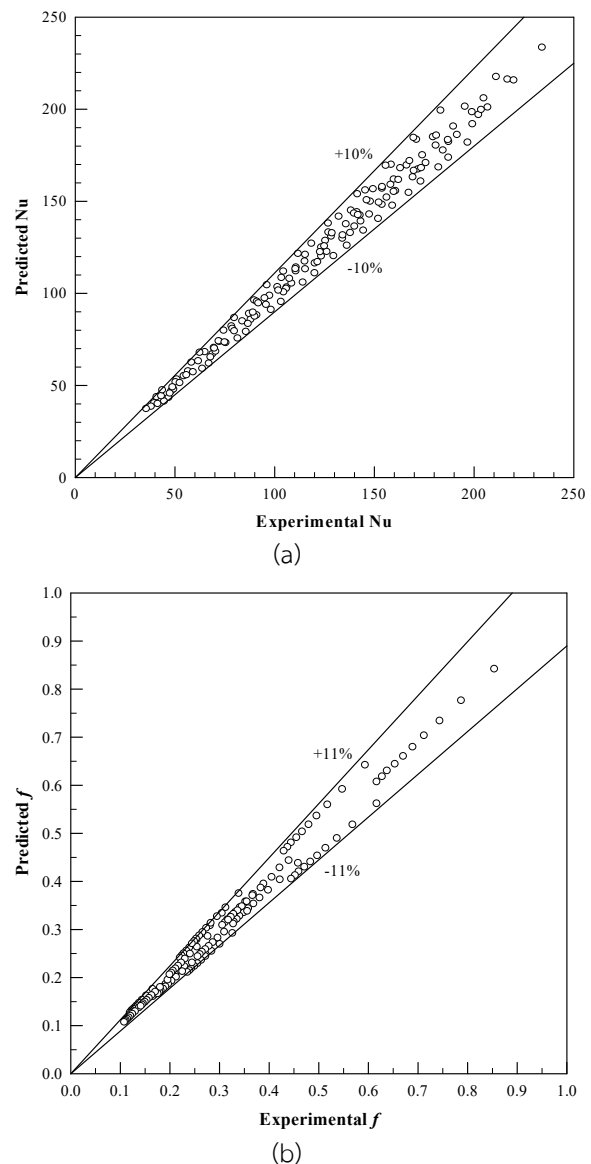


Fig. 8. Predicted data of (a)  $Nu$  and (b)  $f$  versus experimental data for  $45^\circ$  DFTVD.

## 5. Conclusions

Experimental work has been carried out to investigate airflow friction and heat transfer characteristics in a square-duct inserted diagonally with a 45° discrete V-finned tape with V-tip pointing downstream (45° DFTVD) at different *BRs* and *PRs* for the turbulent flow, *Re* from 4000 to 25,000. The 45° DFTVD's parameters including *BRs* and *PRs* affect the flow in the duct leading to increased heat transfer and increased pressure drop. It can be seen that the maximum heat transfer and pressure drop due to the 45° DFTVD is found at the highest *BR* but at the lowest *PR*. For thermal performance comparison, the 45° DFTVD at *PR*=1.5 and *BR*=0.1 yields the highest thermal enhancement factor of about 1.66 at *Re*= 4130. Furthermore, the effect on the performance of the discrete V-finned Tape of the V-tip pointing downstream and upstream was investigated by comparing with a relevant previous study. It was found that changing the V-tip from pointing downstream to upstream increased the thermal enhancement factor by 3%. However, the surplus was insignificant compared with the measurement errors.

## 6. Acknowledgement

We would like to express our thanks to Rajamangala University of Technology Isan , Khonkaen Campus for supporting our work.

### Nomenclature

<i>A</i>	convection heat transfer area of duct, m <sup>2</sup>
<i>BR</i>	fin blockage ratio, <i>e/H</i>
<i>C<sub>p</sub></i>	specific heat capacity of air, J/kgK
<i>D<sub>h</sub></i>	hydraulic diameter of square-duct (=H), m
<i>e</i>	fin height, m
<i>f</i>	friction factor

<i>H</i>	duct height, m
<i>h</i>	average heat transfer coefficient, W/m <sup>2</sup> K
<i>k</i>	thermal conductivity of air, W/mK
<i>L</i>	length of test duct, m
<i>ṁ</i>	mass flow rate of air, kg/s
<i>Nu</i>	Nusselt number
<i>P</i>	fin pitch spacing, m
$\Delta P$	pressure drop, Pa
<i>PR</i>	fin pitch ratio, <i>P/H</i>
<i>Pr</i>	Prandtl number
<i>Re</i>	Reynolds number
<i>Q</i>	heat transfer, W
<i>T</i>	temperature, K
<i>t</i>	thickness of fin, m
<i>U</i>	mean velocity, m/s

### Greek letters

$\alpha$	attack angle of fin, degree
$\eta$	thermal enhancement factor
$\nu$	kinematics viscosity, m <sup>2</sup> /s
$\rho$	density of air, kg/m <sup>3</sup>

### Subscripts

b	bulk
0	smooth duct
conv	convection
i	inlet
o	outlet
bp	blowing power
s	duct surface

## 7. References

- [1] J. Liu, J. Gao, T. Gao, X. Shi, "Heat transfer characteristics in steam-cooled rectangular channels with two opposite rib-roughened walls," *Appl. Therm. Eng.*, 50, pp. 104-111. 2013.
- [2] P. Sriromreun, C. Thianpong, P. Promvong, "Experimental and numerical study on heat

- transfer enhancement in a channel with Z-shaped baffles,” *Int. Commun. Heat Mass Transfer*, 39, pp. 945-952, 2012.
- [3] W.M. Song, J.A. Meng, Z.X. Li, “Numerical study of air-side performance of a finned flat tube heat exchanger with crossed discrete double inclined ribs,” *Appl. Therm. Eng.*, 30, pp. 1797-1804, 2010.
- [4] S. Skullong, P. Promvong, “Experimental investigation on turbulent convection in solar air heater channel fitted with delta winglet vortex generator,” *Chin. J. Chem. Eng.*, 22, pp. 1-10, 2014.
- [5] P. Promvong, “Heat transfer and pressure drop in a channel with multiple 60° V-baffles,” *Int. Commun. Heat Mass Transfer*, 37, pp.835-840. 2010.
- [6] W. Peng, P.X. Jiang, Y.P. Wang, B.Y. Wei, “Experimental and numerical investigation of convection heat transfer in channels with different types of ribs,” *Appl. Therm. Eng.*, 31, pp. 2702-2708, 2011.
- [7] P. Promvong, W. Jedsadaratanachai, S. Kwankaomeng, C. Thianpong, “3D simulation of laminar flow and heat transfer in V-baffled square channel,” *Int. Commun. Heat Mass Transfer*, 39, pp. 85-93, 2012.
- [8] A. Gupta, V. SriHarsha, S.V. Prabhu, R.P. Vedula, “Local heat transfer distribution in a square channel with 90° continuous, 90° saw tooth profiled and 60° broken ribs,” *Exp. Therm. Fluid Sci.*, 32, pp. 997-1010, 2008.
- [9] T. Chompookham, C. Thianpong, S. Kwankaomeng, P. Promvong, “Heat transfer augmentation in a wedge-ribbed channel using winglet vortex generators,” *Int. Commun. Heat Mass Transfer*, 37, pp. 163-166, 2010.
- [10] S. Skullong, S. Kwankaomeng, C. Thianpong, P. Promvong, “Thermal performance of turbulent flow in a solar air heater channel with rib-groove turbulators,” *Int. Commun. Heat Mass Transfer*, 50, pp. 34-43, 2014.
- [11] C. Min, C. Qi, X. Kong, J. Dong, “Experimental study of rectangular channel with modified rectangular longitudinal vortex generators,” *Int. J. Heat Mass Transfer*, 53, pp. 3023-3029, 2010.
- [12] V.S. Hans, R.P. Saini, J.S. Saini, “Heat Transfer and friction factor correlations for a solar air heater duct roughened artificially with multiple V-ribs,” *Solar Energy*, 84, pp. 898- 911, 2010.
- [13] S. Eiamsa-ard, P. Promvong, “Thermal characteristics of turbulent rib-grooved channel flows,” *Int. Commun. Heat Mass Transfer*, 36, pp. 705-711, 2009.
- [14] S. Eiamsa-ard, N. Koolnapadol, P. Promvong, “Heat transfer behavior in a square duct with tandem wire coil element insert,” *Chin. J. Chem. Eng.*, 20, pp. 863-869, 2012.
- [15] P. Promvong, “Thermal performance in square-duct heat exchanger with quadruple V-finned twisted-tapes,” *Appl. Therm. Eng.*, 91, pp. 298-307, 2015.
- [16] P. Promvong, S. Suwannapan, M. Pimsarn, C. Thianpong, “Experimental study on heat transfer in square-duct with combined twisted-tape and winglet vortex generators,” *Int. Commun. Heat Mass Transfer*, 59, pp. 158-165, 2014.

- [17] P. Promvong, S. Skullong, S. Kwankaomeng, C. Thianpong, "Heat transfer in square duct fitted diagonally with angle-finned tape-part 1: experimental study," *Int. Commun. Heat Mass Transfer*, 39, pp. 617-62, 2012.
- [18] P. Promvong, S. Skullong, S. Kwankaomeng, C. Thianpong, "Heat transfer in square duct fitted diagonally with angle-finned tape-part 2: numerical study," *Int. Commun. Heat Mass Transfer*, 39, pp. 625-633, 2012.
- [19] W. Noothong, S. Suwannapan, C. Thianpong, P. Promvong, "Enhanced heat transfer in a heat exchanger square-duct with discrete V-finned tape inserts," *Chin. J. Chem. Eng.*, 23, pp. 490-498, 2015.
- [20] ANSI/ASME, "Measurement Uncertainty," 1986. PTC 19, 1-1985. Part I.
- [21] R. L. Webb, "Principles of Enhanced Heat Transfer," New York, John-Wiley & Sons, 1992.
- [22] F. Incropera, P.D. Dewitt, "Introduction to Heat Transfer," fifth ed., John Wiley & Sons Inc, 2006.
- [23] European Federation of National Associations of Measurement Testing and Analytical Laboratories, "Guide to the Evaluation of Measurement Uncertainty for Quantitative Test Results," Paris, 2006.